On the Inside of Massive Galaxies: The Sloan Lens ACS Survey and Combining Gravitational Lensing with Stellar Dynamics and Stellar Population Analysis

Léon Koopmans[1]
Oliver Czoske[2]

[1] Kapteyn Astronomical Institute, Groningen, the Netherlands
[2] Institut für Astrophysik, Universität Wien, Austria

Our understanding of the structure and formation of early-type galaxies (ETGs) is rapidly evolving, but our inability to disentangle stellar mass from dark matter often prevents direct comparison of galaxy formation models with observations without making strong assumptions, such as for the initial mass function (IMF) or dark matter mass fraction and density profile. As an example, the increase in mass-to-light ratio (M/L) along the Fundamental Plane could be partly due to changes in the structure of the ETGs, but also to a change in the ratio of dark versus stellar mass and even to a change in the stellar M/L with galaxy velocity dispersion (by a steepening of the IMF). We report on ongoing efforts to disentangle the structure of early-type galaxies using gravitational lensing, two-dimensional kinematics and stellar population analysis making use of high-resolution images from HST, integral field spectroscopy from VIMOS, and UVB/VIS spectra from X-shooter.

Background

Understanding the internal structure of massive galaxies, the present-day end-products of galaxy formation, as well as their evolution over cosmic time is important for understanding galaxy formation and the physical processes that shape galaxies.

One of the roadblocks in these studies has been the (often) unknown contribution of dark matter to the mass distribution of galaxies. Historically, galaxy dynamics has been the main diagnostic to determine how matter is distributed in galaxies, but even in the local Universe it has been difficult to disentangle the contributions and relative distributions of baryonic matter (stars and gas) and dark matter; the reason being the notorious mass-anisotropy degeneracy inherent in dynamical analyses. This has led to many claims of the presence or absence of dark matter in early-type galaxies (ETGs), although some were based on assumptions that were hard to justify (e.g., orbital (an)isotropy).

In recent years, substantial progress has been made to remedy these issues, in particular using integral field spectroscopy to map the kinematics of galaxies (velocities and velocity dispersions) in two dimensions (e.g., ATLAS^{3D}; COMA). However, studies remain confined to the relatively nearby Universe, where ETGs can be studied in greater detail and out to larger galactic radii than at larger cosmological distances. Studying the cosmological evolution of galaxy structure remains out of reach using kinematic/dynamic techniques alone, at least until the recently approved European Extremely Large Telescope (E-ELT) and its equivalents in the US are completed in ten years time.

At cosmological distances (say $z \gtrsim 0.1$), massive galaxies may act as gravitational lenses on background sources at higher redshifts. Modelling the shape of strongly gravitationally lensed sources has become a powerful new tool to investigate the structure of the lens galaxies. While the total mass within the Einstein radius (typically 5–10 kpc at cosmological distances) can be measured extremely accurately (to a few percent), lensing analysis alone also suffers from degeneracies, notably the mass-sheet degeneracy, that prevent unambiguous determination of the mass profile. In order to break these degeneracies, additional information or a combination of information from several independent methods is required.

Over the past decade, new techniques have been developed that systematically combine strong gravitational lensing with galaxy dynamics to break the mass-sheet and mass-anisotropy degeneracies (see e.g., Koopmans & Treu, 2002; Treu & Koopmans, 2004). The constraints from the two methods are complementary, making their combination particularly powerful in studying galaxy structure. The combination of a lensing analysis with even a single stellar velocity dispersion measurement allows the total mass-density slope at the Einstein radius to be measured with an accuracy of typically better than 5% out to redshifts of $z \sim 1$ (Koopmans & Treu, 2002; Treu & Koopmans, 2002). The reason is that the mass enclosed by the Einstein radius is accurately determined from the lensing constraints, significantly reducing its degeneracy with the orbital anisotropy.

To further and self-consistently combine these methodologies beyond the early techniques, where the only lensing constraint used was the mass of the ETG, Barnabè & Koopmans (2007) developed fully grid-based lensing and two-integral dynamical models that can describe the combined two-dimensional datasets (i.e. the lensed images along with velocity and velocity dispersion fields) without the usual assumption of spherical symmetry or Jeans modelling. The combined lensing/dynamics analysis yields the total mass distribution. The final piece of information to disentangle the relative contributions of dark and stellar matter in galaxies is stellar population modelling of the galaxy spectrum, which yields the mass-to-light ratio of the stars and information on the initial mass function (IMF), enabling the light distribution to be converted to the stellar mass distribution.

Powerful techniques require equally good data and much of the effort going into the development of the methods has been driven by the powerful instrumentation on 8–10-metre-class telescopes. On the VLT, the VIMOS integral field unit (IFU) instrument has provided two-dimensional kinematic data of a large sample of strong lens systems. More recently, X-shooter has provided exquisite spectral data whose broad wavelength coverage is ideal for detailed stellar population analysis.

In this article we describe some results from the Sloan Lens ACS Survey (SLACS; see Figure 1), in particular focusing on the critical contributions of VIMOS and X-shooter toward breaking degeneracies in the mass models of ETGs, disentangling the stellar and dark matter density profiles and quantifying these as function of galaxy mass and redshift.

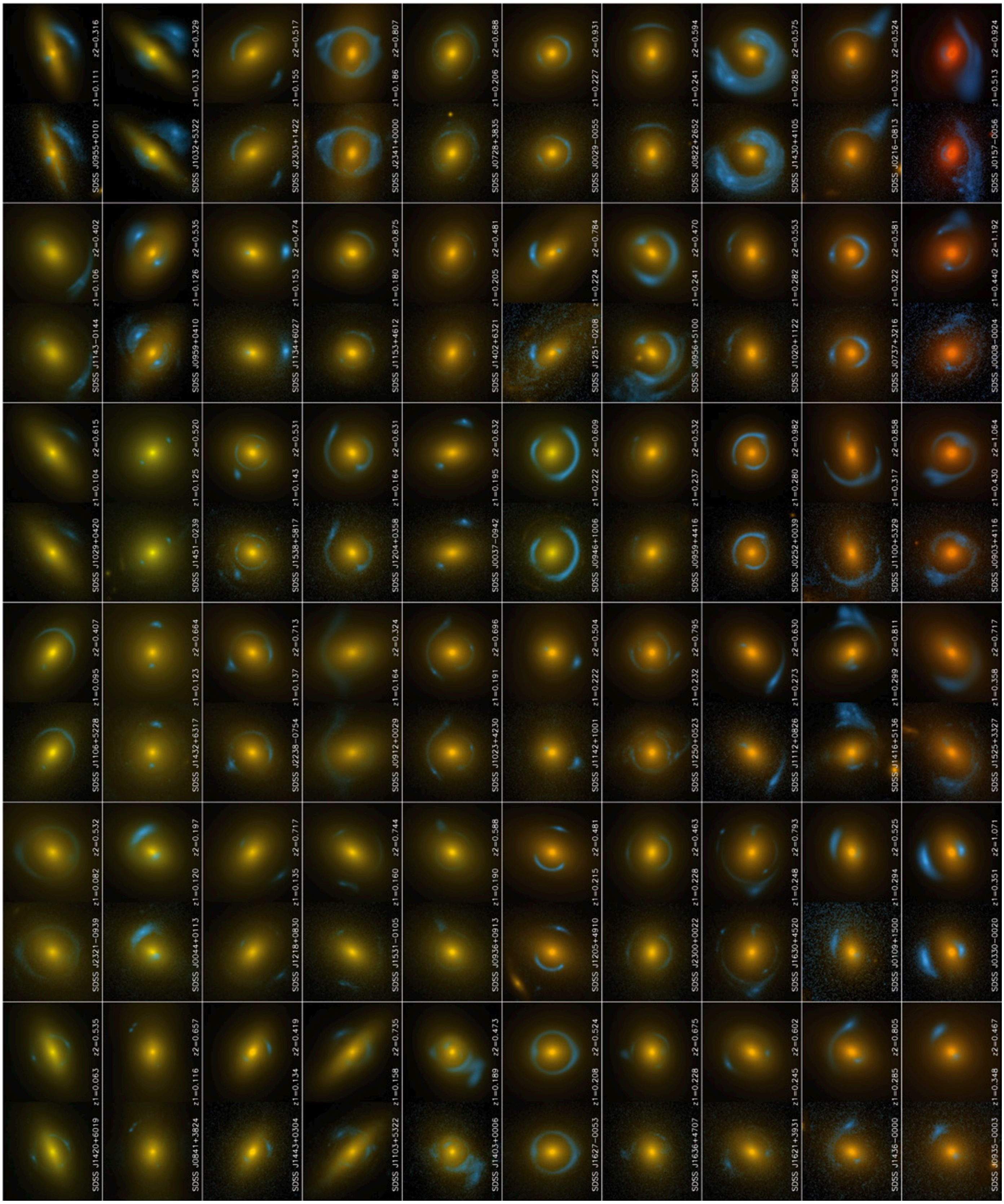
SDSS J0955+0101 z1=0.111 z2=0.316
SDSS J1032+5322 z1=0.133 z2=0.329
SDSS J2303+1422 z1=0.155 z2=0.517
SDSS J2341+0000 z1=0.186 z2=0.807
SDSS J0728+3835 z1=0.206 z2=0.688
SDSS J0029−0055 z1=0.227 z2=0.931
SDSS J0822+2652 z1=0.241 z2=0.594
SDSS J1430+4105 z1=0.285 z2=0.575
SDSS J0216−0813 z1=0.332 z2=0.524
SDSS J0157−0056 z1=0.513 z2=0.924
SDSS J1143−0144 z1=0.106 z2=0.402
SDSS J0959+0410 z1=0.126 z2=0.535
SDSS J1134+6027 z1=0.153 z2=0.474
SDSS J1153+4612 z1=0.180 z2=0.875
SDSS J1402+6321 z1=0.205 z2=0.481
SDSS J1251−0208 z1=0.224 z2=0.784
SDSS J0956+5100 z1=0.241 z2=0.470
SDSS J1020+1122 z1=0.282 z2=0.553
SDSS J0737+3216 z1=0.322 z2=0.581
SDSS J0008−0004 z1=0.440 z2=1.192
SDSS J1029+0420 z1=0.104 z2=0.615
SDSS J1451−0239 z1=0.125 z2=0.520
SDSS J1538+5817 z1=0.143 z2=0.531
SDSS J1204+0358 z1=0.164 z2=0.631
SDSS J0037−0942 z1=0.195 z2=0.632
SDSS J0946+1006 z1=0.222 z2=0.609
SDSS J0959+4416 z1=0.237 z2=0.532
SDSS J0252+0039 z1=0.280 z2=0.982
SDSS J1100+5329 z1=0.317 z2=0.858
SDSS J0903+4116 z1=0.430 z2=1.064
SDSS J1106+5228 z1=0.095 z2=0.407
SDSS J1432+6317 z1=0.123 z2=0.664
SDSS J2238−0754 z1=0.137 z2=0.713
SDSS J0912+0029 z1=0.164 z2=0.324
SDSS J1023+4230 z1=0.191 z2=0.696
SDSS J1142+1001 z1=0.222 z2=0.504
SDSS J1250+0523 z1=0.232 z2=0.795
SDSS J1112+0826 z1=0.273 z2=0.630
SDSS J1416+5136 z1=0.299 z2=0.811
SDSS J1525+3327 z1=0.358 z2=0.717
SDSS J2321−0939 z1=0.082 z2=0.532
SDSS J0044+0113 z1=0.120 z2=0.197
SDSS J1218+0830 z1=0.135 z2=0.717
SDSS J1531−0105 z1=0.160 z2=0.744
SDSS J0936+0913 z1=0.190 z2=0.588
SDSS J1205+4910 z1=0.215 z2=0.481
SDSS J2300+0022 z1=0.228 z2=0.463
SDSS J1630+4520 z1=0.248 z2=0.793
SDSS J0109+1500 z1=0.294 z2=0.525
SDSS J0330−0020 z1=0.351 z2=1.071
SDSS J1420+6019 z1=0.063 z2=0.535
SDSS J0841+3824 z1=0.116 z2=0.657
SDSS J1443+0304 z1=0.134 z2=0.419
SDSS J1103+5322 z1=0.158 z2=0.735
SDSS J1403+0006 z1=0.189 z2=0.473
SDSS J1627−0053 z1=0.208 z2=0.524
SDSS J1636+4707 z1=0.228 z2=0.675
SDSS J1621+3931 z1=0.245 z2=0.602
SDSS J1436−0000 z1=0.285 z2=0.805
SDSS J0935−0003 z1=0.348 z2=0.467

Figure 1 (opposite page). A subsample of 60 SLACS lens systems. For each system, the left panel shows a multi-colour HST image and the right panel shows a reconstruction from the best-fitting lens model.

Finding suitable lenses: the Sloan Lens ACS Survey

Progress in strong gravitational lensing has often been driven by new instrumentation, allowing detailed study of these typically arcsecond-scale systems. The advent of space-based observatories, in particular the Hubble Space Telescope (HST), has allowed optical and infrared images with ~ 0.1 arcsecond resolution, revolutionising the field. Recently, adaptive optics (AO) observations have enabled ground-based telescopes to compete again or even overtake space-based imaging (see e.g., the SHARP projects; Lagattuta et al., 2012; Vegetti et al., 2012). For spectroscopy, 8–10-metre-class telescopes are without competition. IFU observations with the Very Large Telescope (VLT) in particular have made it possible to obtain detailed maps of the kinematic fields of lens ETGs, as we will show.

Gravitational lenses are rare — only a few hundred are known across the entire sky. Early lens searches targeted potentially lensed background sources, and consequently the properties of the lenses were rather heterogeneous. This changed with the advent of the Sloan Digital Sky Survey (SDSS) which took spectra of many millions of targets, among them many ETGs that could act as gravitational lenses. Based on an earlier idea of Warren et al. (1996), the Sloan Lens ACS (SLACS) collaboration (Bolton et al., 2006) searched systematically through the spectra of ETGs in the SDSS database for signs of emission lines coming from a higher redshift. In these cases the 3-arcsecond SDSS fibres ensure a close alignment between a massive ETG and a high-redshift source within 1.5 arcseconds from the ETG. Because the Einstein radius of these systems is often similar to the fibre radius, many of them are excellent strong gravitational lens candidates.

Two more advantages of such a spectroscopic lens search are that the redshifts of the lens and source will both be known without further follow-up, and, in the case of SDSS, a measurement of the stellar velocity dispersion of the ETGs comes for free from these spectra. Given the redshift and the velocity dispersion of the ETG, a simple estimate of the Einstein radius can be made. Nearly 100% of the candidates with an Einstein radius exceeding that of the fibre turned out to be genuine lenses and the overall success rate of the HST follow-up programme exceeded 50%. Extensive follow-up with HST has yielded nearly 100 strong gravitational lens systems with multicolour *V*-, *I*- and *H*-band observations, complete redshift information and stellar velocity dispersions for all systems. A recently completed HST snapshot programme has yielded another ~50 lens systems with somewhat lower stellar velocity dispersions. This programme has collected the most complete and uniform galaxy-scale lens sample to date (Figure 1) with most lenses being luminous red galaxies (LRGs).

Initial results from combined gravitational lens (mass inside the Einstein radius) and kinematic data (velocity dispersion inside the SDSS fibre) turned out to be a powerful constraint on the total density profile (stars plus dark matter) and showed that these ETGs have mass slopes very similar to isothermal spheres (i.e. flat circular velocity curves) and similar to those of spiral galaxies. No evolution with redshift and no correlation with galaxy mass was found in the density profiles, although recent observations may have shown some minor evolution (Bolton et al., 2012). In addition, and probably just as interesting, was the related work on the Fundamental Plane by Bolton et al. (2007), who showed that if one replaces the surface brightness within one effective radius (R_{eff}) by the surface mass density derived from lensing and dynamical models, then the tilt of the Fundamental Plane changes to that derived from the virial theorem. This finding demonstrates that these galaxies are homologous (see e.g., Koopmans et al., 2009) and that the tilt is mostly due to a change in the dark matter content of these galaxies.

Two-dimensional kinematic fields: VLT-VIMOS

To further push the lensing and kinematic analysis and to assess the effects of anisotropy and the non-spherical nature of ETGs in greater detail, a single velocity dispersion measurement is not sufficient. Integral field spectroscopy of 17 SLACS lenses (of which 16 were ETGs) was obtained with the VIMOS IFU on the VLT in 2006–2008, as part of a VLT Large Programme (see Figure 2). Fitting of the spectra with stellar templates yielded two-dimensional kinematic maps of systematic velocity (e.g., due to bulk rotation of the galaxy) and velocity dispersion, typically out to 1 R_{eff}. These data were combined with high-resolution HST imaging of the gravitational-lens configuration and modelled in a fully self-consistent way. Although the results are in remarkable agreement (in general within the errors) with previous results based on simpler analyses, a much more detailed and three-dimensional census was obtained from the selected 16 ETGs. The total mass density profiles (Figure 3) could be compared with the stellar mass density under the assumption of two different stellar IMFs (Chabrier and Salpeter).

The main results that have come out of the VIMOS studies are that ETGs genuinely have total density profiles very close to isothermal, but also that there is intrinsic scatter between density profiles of order 10%, consistent with studies in the nearby Universe. A small but interesting correlation is found between the density slope and the stellar mass density, which may be a result of their formation (e.g., adiabatic contraction). Another major result is that, for a fixed IMF along the mass sequence, the deviation between the total mass-density profile and that for the stars increases rapidly. Assuming the IMF is not varying (this question will be addressed later), this implies that the dark-matter content of ETGs within 1 R_{eff} is not only non-negligible but can even dominate for the most massive systems, with velocity dispersion $\sigma > 300$ km/s.

The inferred increase in dark matter content in the inner parts of ETGs is consistent with models where feedback increases for increasingly more massive ETGs, either through supernova or active galactic nucleus feedback (Hopkins et al., 2006). However, it should be kept in mind that a similar increase can also be caused by a change in the IMF for low-mass stars ($< 0.5\ M_{\odot}$; van Dokkum &

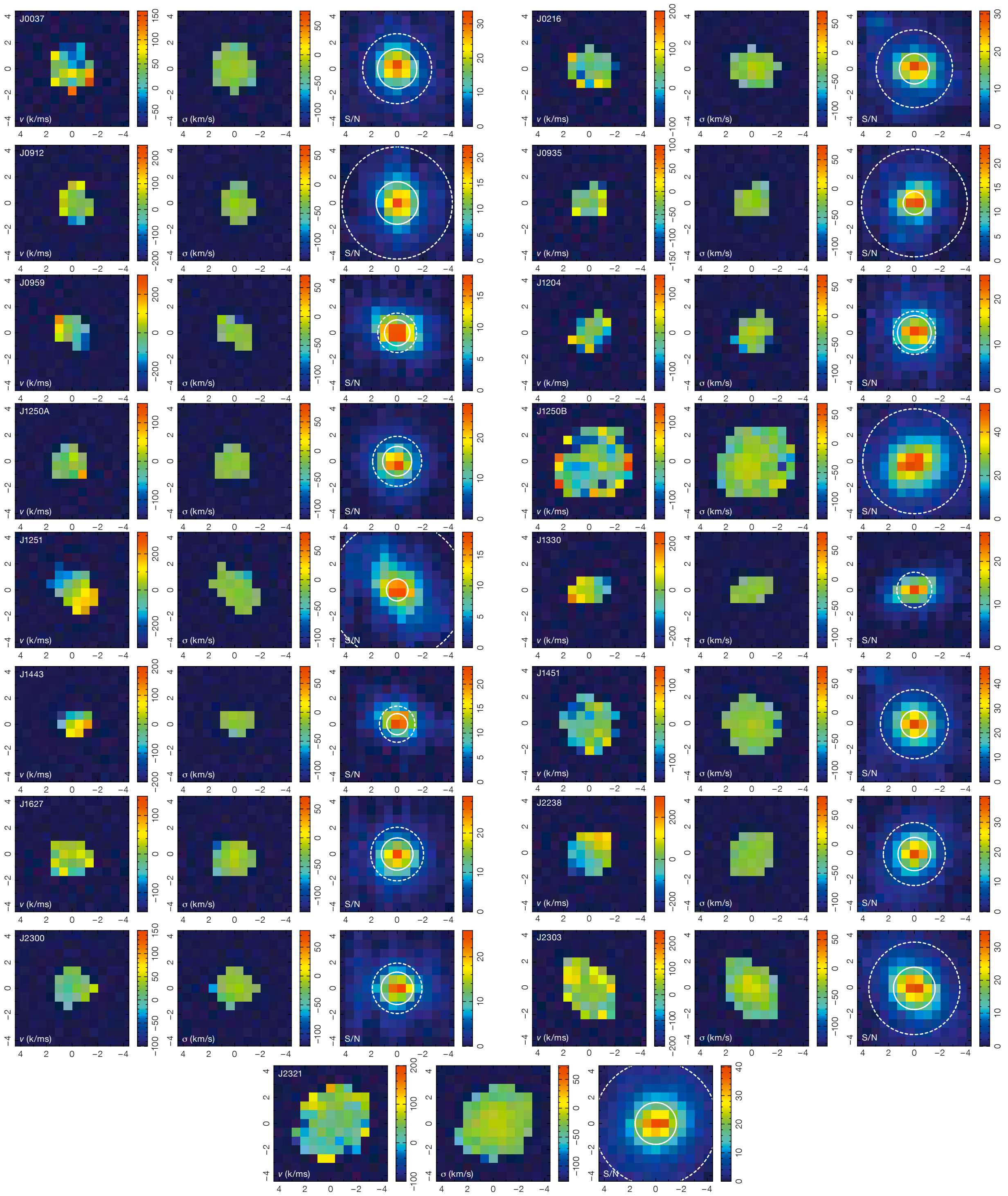

Figure 2. Kinematic maps for 17 SLACS lens systems as derived from VIMOS/IFU observations. For each system, the left panel shows the systematic velocity (with respect to the mean redshift of the lens galaxy), the middle panel the velocity dispersion and the right panel the signal-to-noise (S/N) ratios of the spectra in the stacked datacube. Kinematic measurements were obtained for spectra with S/N > 8 (per 0.65 Å pixel). From Czoske et al. (2012).

Conroy, 2010). This could indeed work for the lower-mass ETGs as can be seen in Figure 3, because the shapes of the stellar and total density profiles are relatively similar up to a constant within 1 R_{eff}. Steepening the low-mass end of the IMF could increase the stellar mass content of these galaxies to a level that dark matter is no longer needed, but in general this requires an IMF that is steeper than the Salpeter IMF. In many cases, however, scaling of the stellar mass profile does not match the total density profile, reflecting the fact that a steepening of

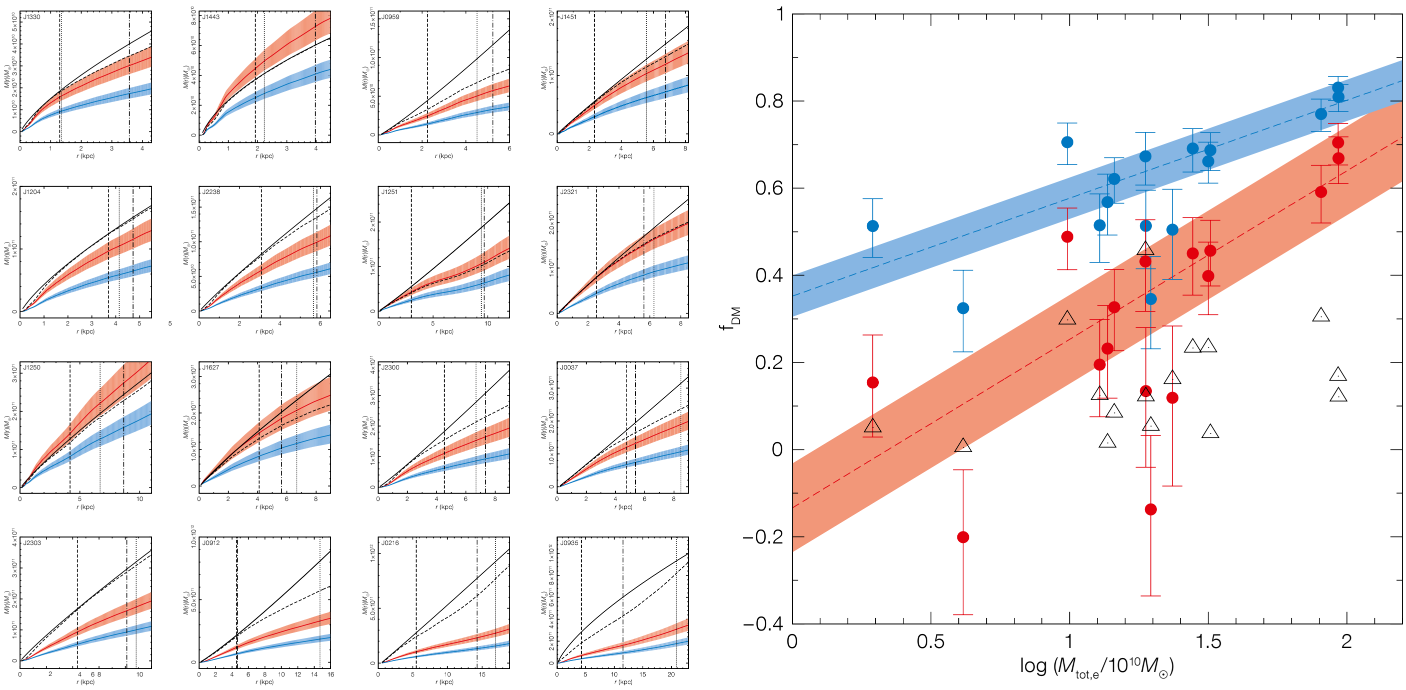

Figure 3. Left: Spherically averaged mass distributions for the 16 early-type galaxies in the SLACS/VIMOS sample, arranged by increasing galaxy mass. The total mass profiles, as derived from the lensing/kinematics analysis, are shown by solid black lines. Stellar mass profiles have been derived for two different IMFs: Salpeter (red) and Chabrier (blue). The dashed black line rescales the luminous mass profile to its maximum value consistent with the total mass distribution (the maximum-bulge hypothesis). Right: Dark matter fractions (f_{DM}) *versus* total mass enclosed within the three-dimensional effective radius for the 16 early-type galaxies in the sample, computed for Salpeter (red) and Chabrier (blue) IMFs. Lower limits for the dark matter fractions were obtained from the maximum-bulge hypothesis (open triangles). From Barnabè et al. (2011).

the IMF cannot be the sole cause of the change in M/L in ETGs. In fact, models with constant M/L can also be excluded for many other lens ETGs for which kinematic data are available, showing the strength of combining these two techniques. However, some degeneracies between stellar and dark matter mass remain.

Stellar populations and the initial mass function: XLENS with X-shooter

Our ability to measure the stellar IMF of these galaxies is one final piece in the puzzle posed by disentangling the fraction of the total mass in ETGs that is contained in dark matter. Again, the combination of lensing and dynamics gives very interesting clues. In Treu et al. (2010) it was found that a full analysis of 53 SLACS ETGs indicates that a Salpeter IMF fits the data best and that “light” IMFs (e.g., Chabrier, Kroupa) can be excluded. This agreed well with the later result by, for example, van Dokkum & Conroy (2010) that the spectra of ETGs seem to show absorption-line equivalent widths typical for low-mass stars and thus are only consistent with more bottom-heavy IMFs. A complementary analysis by Auger et al. (2010) based on their full structure seems to confirm that light IMFs are inconsistent with the kinematics of these ETGs.

Another tantalising result from SLACS was that the IMF seems to steepen with galaxy mass, although this was only found at the 2σ confidence level (Treu et al., 2010). In order to investigate this effect in greater detail we started the XLENS survey, which follows up a subsample of ten lenses with X-shooter covering the full ultraviolet to near-infrared (UV–NIR) wavelength range in order to measure the equivalent widths of several absorption lines (Na I, FeH, TiO_2, etc.) that are especially sensitive to low-mass stars. Based on a pilot programme, Spiniello et al. (2011) combined kinematic constraints from X-shooter data with lensing data of the Horseshoe lens system (Figure 4) as well as spectral energy distribution (SED) fitting to disentangle the stellar and dark matter distributions. Although lighter IMFs are harder to exclude due to degeneracies between the stellar and dark matter halo mass distributions, IMFs as steep as Salpeter (slope 2.35) were allowed. Also mass-function slopes steeper than 3.0 were excluded, based simply on the total enclosed mass within the Einstein radius of the system as well as the velocity dispersion profile (Spiniello et al., 2011).

New X-shooter data on the sample of ten systems continues to be obtained. First results were presented in Spiniello et al. (2012) based on one extremely interesting XLENS system (Figure 5) that shows very deep Na I and TiO_2 lines, which are both regarded as potential indicators of a population of low-mass stars (< 0.3 $M_{\odot}$). Naively therefore, this system should have a very steep IMF, which can however be excluded with high confidence for slopes exceeding 3.0. Combined with a larger sample of spectra from the SDSS (Figure 5), it was also shown that these lines deepen with increasing stellar velocity dispersion, suggesting some mild steepening of the IMF, in agreement with the work of Treu et al. (2010). Theoretical work by, for example, Hopkins (2012)

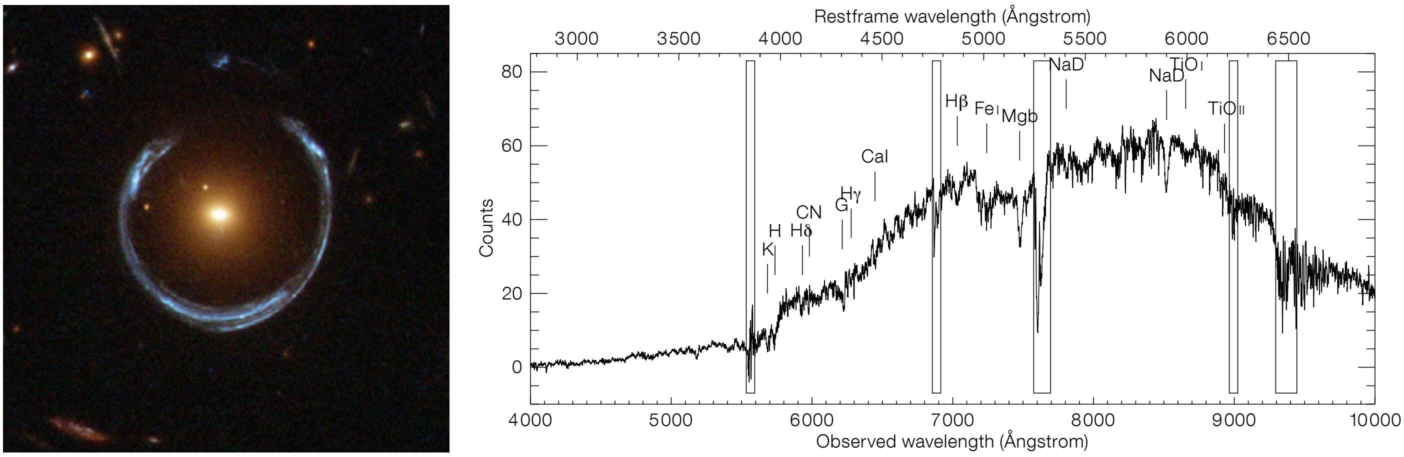

Figure 4 (above). Left: HST image of SDSS J1148+1930 (The Cosmic Horseshoe). Right: X-shooter spectrum of SDSS J1148+1930, covering the UVB and VIS arms. Several spectral features are marked, as are the positions of telluric absorption features and sky lines (boxes). From Spiniello et al. (2011).

Figure 5 (below). Index–index plots of ~250 ETGs from the SDSS, colour-coded by velocity dispersion. Lines that are sensitive to low-mass stars ([MgFe] (Gonzalez, 1993), TiO_2, Na I) tend to deepen with increasing velocity dispersion, indicative of a steepening of the low-mass IMF slope with galaxy mass (panels b and c). Various IMF slopes are plotted (C = Chabrier). The bottom-right panel (d) shows the correlation between the Na I and TiO_2 indicators, displaying a modest steepening of the IMF from Salpeter (slope of 2.35) to an IMF with a slope slightly less than 3.0. From Spiniello et al. (2012).

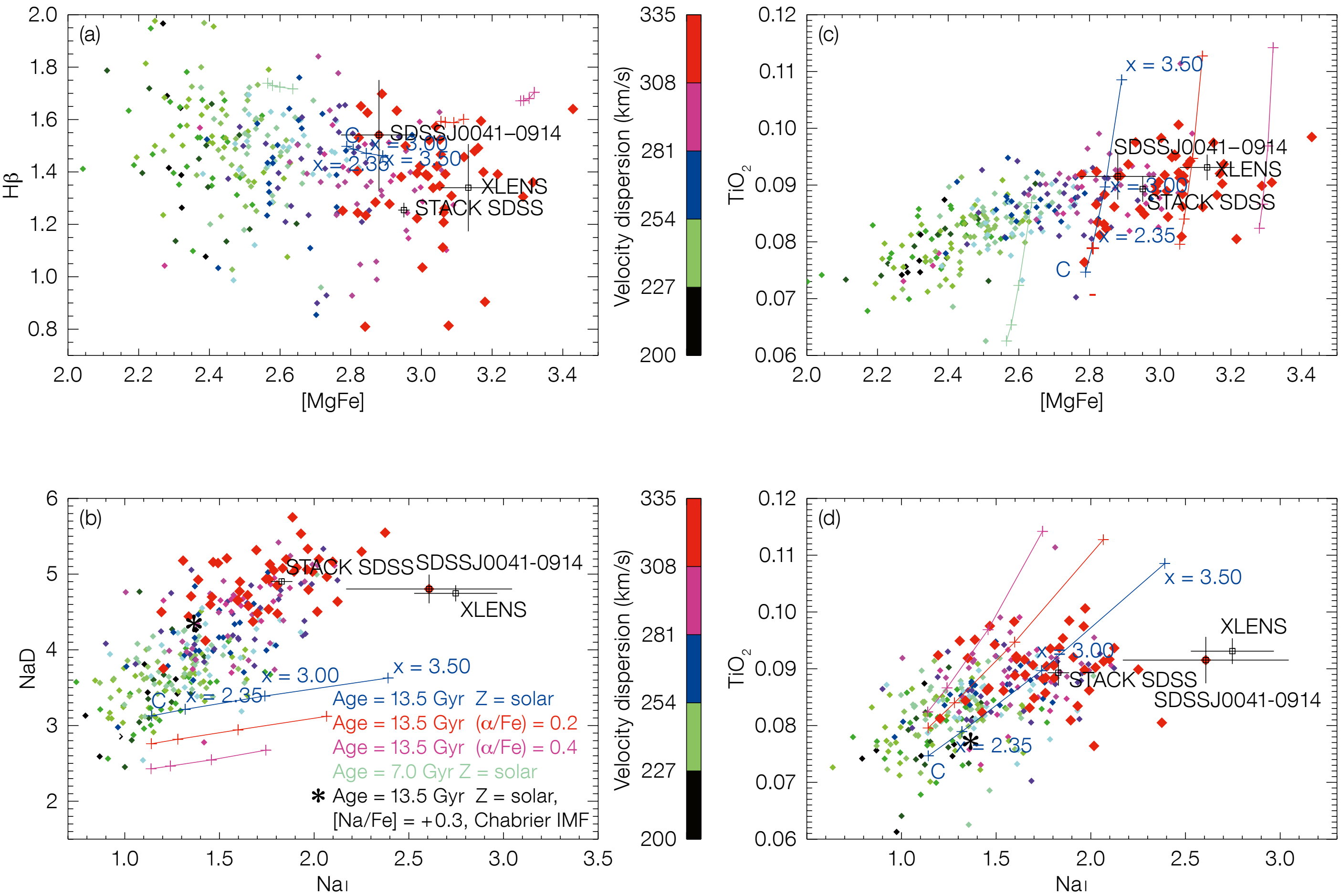

seems to be able to explain this result based on arguments of gas density during star/galaxy formation, but a detailed comparison between observations and theory remains to be done.

Future work

Accurate knowledge of the total mass of a galaxy is essential for disentangling the distributions of stellar and dark matter within it, as it breaks many of the degeneracies in mass models based on stellar kinematics. The technique of combining kinematics and gravitational lensing has been used extensively by the SLACS collaboration to arrive at a number of interesting results on the mass profiles of galaxies, limits on their dark matter content, as well as on the Fundamental Plane and the stellar IMF, as discussed in this article. More recently this analysis has been further extended by including constraints on the stellar IMF from broadband stellar SEDs and spectra.

Two-dimensional kinematics obtained with VIMOS on the VLT in combination with gravitational lensing has been shown to be powerful at modelling the mass distributions in elliptical galaxies beyond the local Universe. The next generation of integral field spectrographs both at the VLT and the E-ELT will further push the limits of applicability of this technique and allow the study of the evolution of the structure of ETGs over a fair fraction of the age of the Universe.

X-shooter will continue to play a crucial role as it allows full ultraviolet to near-infrared spectral coverage in one go; this is critical because the data provide not only the kinematics (from lines in the optical) but also equivalent widths of absorption lines in the infrared that are indicators of low-mass stars and hence can constrain the slope of the IMF. Much work is currently being done in these studies worldwide and we expect to be able to make a much stronger statement in the near future, based on these X-shooter data on a substantial sample of ETGs from SLACS, concerning the contribution of stars (i.e. their IMF) to the mass of ETGs. These results should also shed more light on the tilt of the FP, as well as on their formation history (and feedback) within massive dark matter haloes.

With the recent discovery of ~ 50 more SLACS lenses — extending the mass range down to ~ 150 km/s systems, well below the knee of the mass function of ETGs — we expect even more discoveries in the coming years that will allow a complete census of the internal structure, formation and evolution of ETGs and the successful SLACS saga to continue.

References

Auger, M. et al. 2010, ApJ, 721, L163
Barnabè, M. & Koopmans, L. V. E. 2007, ApJ, 666, 726
Barnabè, M. et al. 2011, MNRAS, 415, 2215
Bolton, A. S. et al. 2006, ApJ, 638, 703
Bolton, A. S. et al. 2007, ApJ, 665, 105
Bolton, A. S. et al. 2012, arXiv:1201.2988
Czoske, O. et al. 2012, MNRAS, 419, 656
Gonzalez, J. J. 1993, PhD Thesis, Univ. California, Santa Cruz
Hopkins, P. F. et al. 2006, ApJS, 163, 1
Hopkins, P. F. 2012, MNRAS, 423, 2037
Koopmans, L. V. E. & Treu, T. 2002, ApJ, 568, L5
Koopmans, L. V. E. et al. 2006, ApJ, 649, 599
Koopmans, L. V. E. et al. 2009, ApJL, 703, L51
Lagattuta, D. J. et al. 2012, MNRAS, 424, 2800
Spiniello, C. et al. 2011, MNRAS, 417, 3000
Spiniello, C. et al. 2012, ApJ, 753, 32
Treu, T. & Koopmans, L. V. E. 2002, ApJ, 575, 87
Treu, T. et al. 2010, ApJ, 709, 1195
van Dokkum, P. G. & Conroy, C. 2010, Nature, 468, 940
Vegetti, S. et al. 2012, Nature, 481, 341
Warren, S. J. et al. 1996, MNRAS, 278, 139

ESO/SOAR/NASA

This false colour picture of the galaxy cluster ACT-CL J0102–4915 combines *R*-, *i*- and *z*-band images taken with FORS2 on the VLT, *griz*-band images from the SOAR Telescope and X-ray observations of the hot gas from NASA's Chandra X-ray Observatory. The galaxy cluster is probably the most massive, hottest, most X-ray luminous and brightest Sunyaev-Zeldovich effect cluster currently known at a redshift greater than 0.6 and so was named *El Gordo*. See Release eso1203 for more details.